Magnetic anisotropy and relaxation behavior of six-coordinate tris(pivalato)-Co(II) and -Ni(II) complexes

Shu-Yang Chen,^a Hui-Hui Cui,^a Yi-Quan Zhang,^{b*} Zhenxing Wang,^{c*} Zhongwen Ouyang,^c Lei Chen,^d Xue-Tai Chen,^{a*} Hong Yan,^a Zi-Ling Xue^e

Abstract: Experimental and theoretical studies of the magnetic anisotropy and relaxation behavior of six-coordinate tris(pivalato)-Co(II) and -Ni(II) complexes (NBu4)[M(piv)3] (piv = pivalate, M = Co, 1; M = Ni, 2), with coordination configuration at the intermediate between octahedron and trigonal prismatic geometry, are reported. The direct-current magnetic data and high-frequency and -field EPR spectra (HFEPR) of 1 have been modeled by a Hamiltonian considering the first-order orbital angular momentum, while the spin Hamiltonian was used to interpret the data of 2. Both 1 and 2 show the easy-axis magnetic anisotropies, which are further supported by *ab initio* calculations. The alternative-current (ac) magnetic susceptibilities reveal the slow magnetization relaxation at an applied dc field of 1000 Oe in 1, which is characteristic of a field-induced single-molecule magnet (SMM), but

-

^aState Key Laboratory of Coordination Chemistry, School of Chemistry and Chemical Engineering, Nanjing University, Nanjing 210023, China. E-mail: <u>xtchen@nju.edu.cn</u>.

^bJiangsu Key Laboratory for NSLSCS, School of Physical Science and Technology, Nanjing Normal University, Nanjing 210023, China. Email: zhangyiquan@njnu.edu.cn

^cWuhan National High Magnetic Field Center, Huazhong University of Science and Technology, Wuhan 430074, China. Email: zxwang@hust.edu.cn

^dSchool of Environmental and Chemical Engineering, Jiangsu University of Science and Technology, Zhenjiang 212003, China.

^eDepartment of Chemistry, University of Tennessee, Knoxville, Tennessee 37996, USA.

[†]Electronic supplementary information (ESI) available: XRD patterns, calculations results and magnetic data.

2 does not exhibit the single-ion magnet property at 1.8 K. The detailed analyses of the relaxation times show the dominant contribution of a Raman process for the spin relaxation in 1.

Introduction

Single-molecule magnets (SMMs) are molecular species retaining the magnetization after removing the external magnetic field at low temperature due to the existence of energy barrier, which prevents the reversal of magnetic moment. Such molecular nanomagnets have showed potential applications in quantum computation, high density information storage, and molecular spintronics. Initially much efforts were devoted to polynuclear 3d-based SMMs. More recently, SMM behaviors have also been demonstrated in metal complexes containing single paramagnetic lanthanide, actinide, or transition metal ion, which are termed as single-ion magnets (SIMs). Since the first Fe(II)-SIM complex was reported by Long et al. in 2010, numerous d-ion SIMs have been found, including Mn(III, IV), Fe(I, II, III) 6.8 Co(I, II), 11 Ni(I, II), 12 Cu(II) 3, Cr(II), 14 and Re(IV). 15 Co(II)-SIMs constitute the largest family because of their non-integer ground-state spin and the large magnetic anisotropy.

Magnetic anisotropy is the most important cause for the slow relaxation of the magnetization. The advantage of the SIMs is that the magnetic anisotropy can be easily tuned by the interplay between ligand field splitting and spin-orbit interaction. For the majority of d-ion complexes, the first-order orbital momentum is usually quenched by the ligand field. Thus, magnetic anisotropy arises from the coupling

between a non-degenerate electronic ground state and orbitally degenerate excited state. Since these couplings are usually weak, the resulting magnetic anisotropy is mostly small, which can be modeled as zero-field spitting using axial and rhombic parameters D and E, respectively. However, in some cases where the orbital momentum is unquenched or just partially quenched as in the case of six-coordinate Co(II) complexes, the first-order spin-orbital coupling occurs and contributes to large magnetic anisotropy. In these cases, the magnetic anisotropy cannot be modeled by the spin-only Hamiltonian with the D and E parameters.

The coordination configurations of the reported Co(II)-SIMs vary along with the coordination number from two to eight. 9-11 Since the first example of six-coordinate field-induced Co(II) SIMs was reported, 10a many Co(II) complexes with octahedral 10 or trigonal prismatic geometries, 10j,11 which exhibit slow magnetic relaxation have been reported. Compared with the common octahedral geometry, 10 a trigonal prism is a better coordination geometry leading to SIMs with slow magnetic relaxation even under zero external static de field due to the large easy-axis magnetic anisotropy. 11 For example, Gao et al. have reported a series of mononuclear, six-oxygen-coordinated Co(II) complexes with distorted trigonal prismatic geometry and large barriers in the range of 26.6–102.8 cm⁻¹. 11a,11b Winpenney et al. have also reported a Co(II) cage complex with a trigonal prismatic configuration surrounded by six nitrogen atoms, showing SIM behavior with high spin-reversal barrier of 152 cm⁻¹. 11c

The magnetic anisotropies of the Ni(II) complexes have been studied to a lesser extent compared to Co(II) complexes. 16-18 The mostly employed technique is the

magnetometry. However, in the absence of the confirmative data from other physical techniques and theoretical calculations, the reliability of the results, especially the sign of the magnetic anisotropy derived, may be questioned. High-frequency and -field EPR spectroscopy (HFEPR) has been successfully used to probe the magnetic anisotropy of Ni(II) complexes of various coordination spheres and geometries. ¹⁷⁻¹⁸ However, the examples of Ni(II)-SIMs are rarely, which include two, six-coordinate octahedral Ni(II) complexes and a mononuclear Ni(II) complex with trigonal bipyramidal geometry. ^{10b-10d}

With the aim to investigate the effect of coordination geometry on the magnetic anisotropy and relaxation behavior, we have investigated the direct-current (dc) and ac magnetic properties of two mononuclear Co(II) and Ni(II) complexes $(NBu_4)[M(piv)_3]$ (piv = pivalate, M = Co, 1; M = Ni, 2) with a coordination configuration at the mid-point between octahedron and trigonal prismatic geometry. The dc magnetic data and high-frequency and -field EPR spectra show their easy-axis magnetic anisotropy, which have been supported by theoretical calculations at the XMS-CASPT2 level. The alternative-current magnetic susceptibility data show that 1 is a field-induced single-ion magnet, while 2 does not exhibit the SIM behavior.

Experimental section

General information

Complexes 1 and 2 were prepared according to the reported procedures. ¹⁹ Their identities were confirmed by elemental analyses (CHN) performed on an Elementar

Vario ELIII elemental analyzer and the infrared spectra measured on a Tensor 27 FT-IR spectrometer using KBr pellets in the range of 400-4000 cm⁻¹. The polycrystalline samples of **1** and **2** for magnetic and HFEPR studies were characterized by powder X-ray diffraction patterns recorded on a Bruker D8 ADVANCE X-ray powder diffractometer in the 2θ range of 5-50° at room temperature (Figs. S1-S2, ESI). HFEPR experiments: Zhengxing: Please add these.

Magnetic measurements

Magnetic measurements were performed on polycrystalline samples of 1 and 2 restrained in a frozen eicosane matrix using a Quantum Design SQUID VSM magnetometer. Direct-current (dc) magnetic data were recorded at fields up to 7 T in the range of 2.0-300 K. Alternative-current (ac) susceptibility measurements were carried out under an oscillating ac field of 2 Oe and ac frequencies ranging from 1 to 1000 Hz. Data were corrected for diamagnetism using Pascal constants and a sample holder correction.

Results and discussion

Structural features

The crystal structures of **1** and **2** have already been reported.¹⁹ Their main structural aspects related to the magnetic properties are emphasized here. The structures of the anionic portions of **1** and **2** are presented in Fig. 1. They are isostructural with the central metal ion displaying a six-coordinate geometry, in which

three pivalato anions are coordinated as bidentate ligands with a cute bite angle 61.86(8), 62.18(8), $62.00(8)^{\circ}$ for 1 and 60.68(1), 61.48(1), $62.54(2)^{\circ}$ for 2. The M-O distances are in the range of 2.105(2)-2.147(2) Å in 1 and 2.045(4)-2.108(4) Å in 2. The six coordinated oxygen atoms can be viewed as in two parallel upper and lower planes with a dihedral angle is 2.44° (1) and 1.79° (2). The twist angle φ (Fig. 2a), defined as the rotation angle of one coordination triangle away from the eclipsed configuration to the other, is 60° for an ideal octahedron and 0° for an ideal trigonal prism, respectively. The angle φ and the tilted angle α of the two planes (Fig. 2b) are 28.71°, 5.74° in 1 and 28.08°, 4.95° for 2. Therefore the coordination geometry in both complexes can be regarded as being at the midpoint of the octahedron and trigonal prismatic geometry. In order to further evaluate the degree of the structural distortion, a continuous shape measurement analyses were performed using the SHAPE program.²⁰ The calculated results can provide an estimate of the distortion degree from the possible ideal structure, and the zero value corresponds to the ideal polyhedron. The obtained values relative to the ideal octahedron and trigonal prismatic geometry are 7.064, 9.337 for 1 and 6.561, 11.090 for 2, respectively. The two values are rather large, suggesting the great deviations of 1 and 2 from the two ideal structural configurations. The metal ions are well-separated for the shortest intermolecular Co---Co distances of 7.46 Å (1) and 7.50 Å (2), thus precluding any prominent intermolecular magnetic interactions.

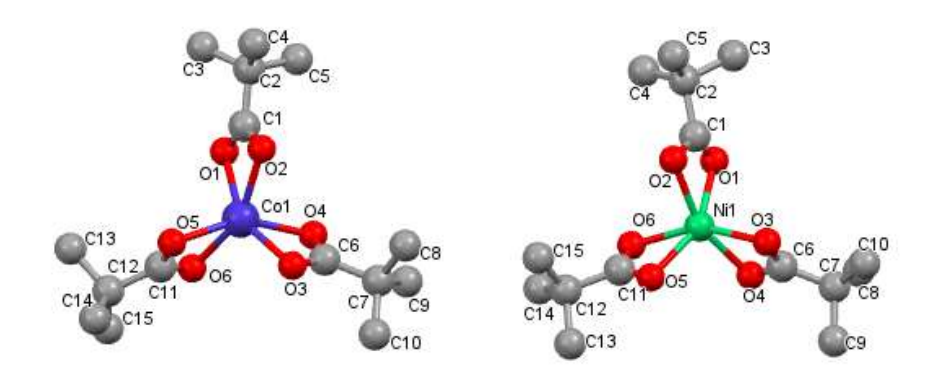


Fig. 1 Structures of the anions in 1 (left) and 2 (right)

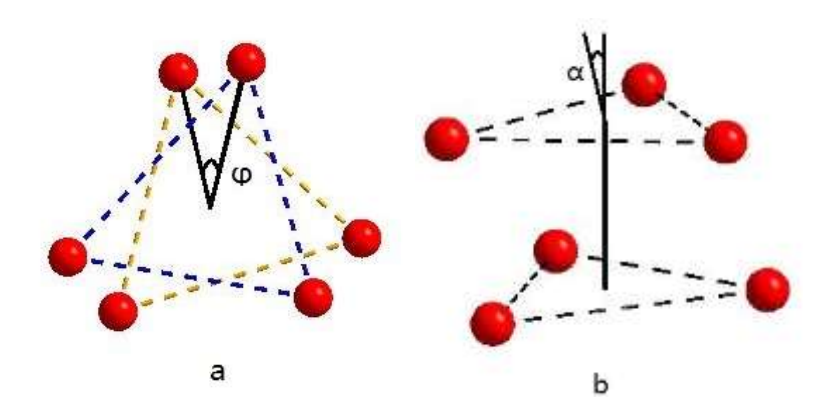


Fig. 2 Twist angles (a) and tilted angles (b) of the coordination polyhedron with respect to ideal prismatic symmetry.

Magnetic anisotropy of (NBu₄)[Co(piv)₃] (1)

Magnetic anisotropy of **1** has been studied by dc magnetic measurements, HFEPR and theoretical calculations. Variable-temperature dc magnetic susceptibilities were measured for the polycrystalline sample of **1**, which had been characterized by powder X-ray diffraction (Fig. S1). The resulting $\chi MT vs T$ plot is typical for a mononuclear Co(II) system with an orbital contribution to the magnetic moment. As shown in Fig. 3, the χMT value at 300 K is 3.00 cm³ K mol⁻¹, larger than the expected value of 1.875 cm³ K mol⁻¹ for one isolated high spin Co(II) ion center (S = 3/2, g = 3/2, g

2.0), indicative of the strong oribital contribution. ^{9-11,21} Upon cooling from 300 K, the $\chi_M T$ value decreases gradually to the minimum value of 1.77 cm³ K mol⁻¹ at 2.0 K. As reported in other six-coordinate Co(II) complexes, ^{9-11,21} such downturn indicates the presence of the strong orbital contribution in **1**, rather than the intermolecular interactions due to the long intermolecular distance between the Co(II) ions. The field-dependent magnetizations of **1** were measured from 1 to 7 T dc field at 2.0, 3.0, and 5.0 K (Fig. 3b). With the increase of the magnetic field, the magnetization continuously increases and reaches 2.25 $N\beta$ at 7 T at 2.0 K, smaller than the expected value of 3.0 $N\beta$ (g = 2.0). The high-field non-saturation also suggests the presence of significant magnetic anisotropy.

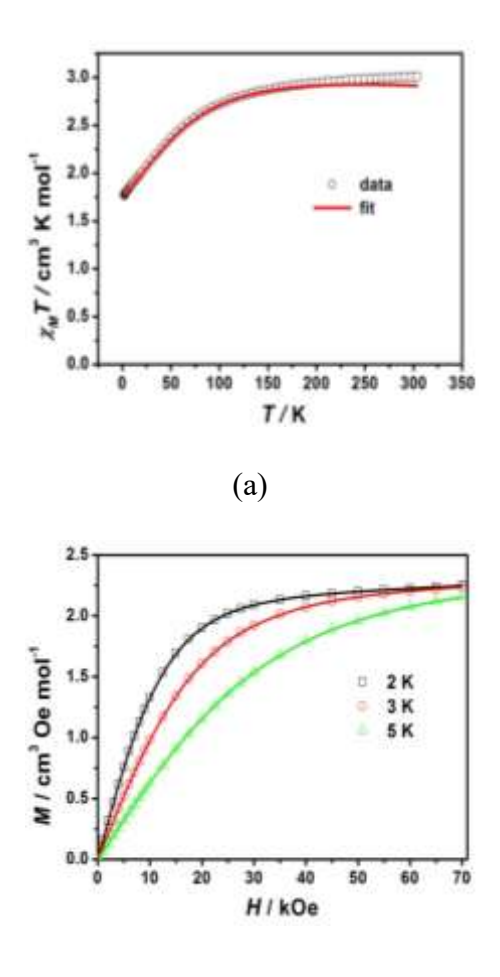


Fig. 3 Variable-temperature dc susceptibility data under an applied dc field of 1000 Oe (a) and field dependent magnetizations (b) for **1**. Solid red lines indicate the best fits with the *PHI* program.²³

In the six-coordinate Co(II) system such as 1, where the unquenched orbital moment leads to the strong orbital contribution to the magnetic moment,²² the fitting of the magnetic data could not yield the sign of the magnetic anisotropy. As pointed out by Palli^{10k,10l} and Chilton,^{10m} a joint analysis of magnetic data with other spectroscopic data such as EPR should be performed. Thus, HFEPR spectra were measured for the polycrystalline sample of 1 at 10 K under different frequencies in the range of 50.8-428.5 GHz (Fig. 4). All the spectra present three main features, corresponding to the effective g values of $g_{x,eff} = 2.42$, $g_{y,eff} = 2.80$ and $g_{z,eff} = 6.57$ with the effective spin $S_{eff} = 1/2$. This pattern is consistent with easy-axis magnetic anisotropy of 1 with significant rhombic component.

The commonly used zero-field splitting parameters D and E cannot be used to present the single-ion magnetic anisotropy in the six-coordinate Co(II) complexes with easy-axis magnetic anisotropy. The most trustworthy treatment of the dc data is the general Hamiltonian shown in equation 1, which takes into account the treatment of the first-order orbital angular momentum of Co(II).

$$\hat{H} = \sigma \lambda \hat{L} \cdot \hat{S} + \sigma^2 (B_2^0 (3\hat{L}_z^2 - \hat{L}^2) + \frac{B_2^2}{2} (\hat{L}_+^2 + \hat{L}_-^2)) + \mu_B (\sigma \hat{L} + 2\hat{S}) \cdot H$$
 (1)

where σ represents a combined orbital reduction parameter $\sigma = -A \cdot \kappa$, λ is the spin-orbit coupling constant, B_2^0 and B_2^2 are crystal field parameters (CFPs). 22,23 The easy-axis magnetic anisotropy showed by EPR indicates that B_2^0 should be negative. The simultaneous fit of the magnetic susceptibilities and magnetization data using the PHI program²³ gives $\lambda = -130.0(1)$ cm⁻¹, $\sigma = -1.25(0)$, $B_2^0 = -90.1(1)$ cm⁻¹, and $B_2^2 = -90.1(1)$ cm⁻¹ 58.5(1) cm⁻¹. Based on these Hamiltonian parameters, we can calculate the corresponding effective g values of the ground Kramers doublet with the effective spin $S_{eff} = 1/2$, $g_{x,eff} = 2.46$, $g_{y,eff} = 3.33$ and $g_{z,eff} = 6.22$. This calculated pattern is similar to that observed by EPR spectra. Furthermore, the first excited state is predicted by PHI program²³ to be 158 cm⁻¹ higher than the ground state, which agrees well with the value calculated by XMS-CASPT2/RASSI²⁴ using the MOLCAS 8.2 program²⁵ (167.6 cm⁻¹, see below). Using $\lambda = -130.0$ cm⁻¹ and $\sigma = -1.25$ obtained from fitting of the magnetic data, we could simulate the HFEPR spectra of 1 by PHI program²³ with $B_2^0 = -107.6$ cm⁻¹ and $B_2^2 = 30.0$ cm⁻¹ (Fig. 4). This consistency between magnetic data and HFEPR confirms the easy-axial nature of magnetic anisotropy.

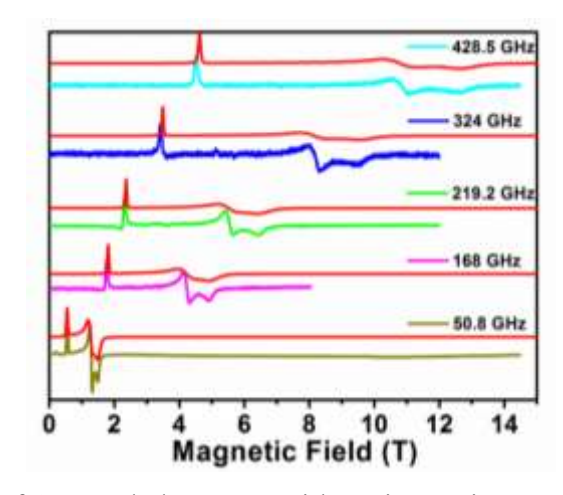


Fig. 4 HFEPR spectra of **1** recorded at 10 K with various microwave frequencies. The red lines represent the best fit obtained by using *PHI*.²³

In order to get further insight into the electronic structure of **1**, theoretical calculations at XMS-CASPT2²⁴ level were carried out using the MOLCAS 8.2 program package.²⁵ Calculation details are given in ESI. The energies of the spin-free states and spin-orbit states were calculated for **1**, which are listed in Tables S1-S3. The energy difference (447.1 cm⁻¹) between the lowest two spin-free states (Table S1) is larger than that between the lowest two spin-orbit states (167.6 cm⁻¹, Table S3). However, the spin-orbit ground state is composed of the lowest three spin-free states, not just formed from the ground one (Table S2). These suggest that there is very strong first-order spin-oribital coupling in **1** and zero-field splitting parameters *D* and *E* cannot be used to depict its magnetic anisotropy. The calculated S = 1/2 effective *g*-values of the ground state Kramers doublet of the Co^{II} of **1**, $g_x = 2.194$, $g_y = 3.345$, and $g_z = 6.835$, are close to those from EPR spectra and magnetic data. The calculated orientations of the g_x , g_y , g_z (hard axis) of the ground doublet on the Co^{II} ion were shown in Fig. S4. Furthermore, the magnetic susceptibilities of **1** were also calculated

as shown in Fig. S5, which are comparable to the experimental curve.

These results support the negative sign of magnetic anisotropy in 1. The same negative anisotropy has been reported for the six-coordinated Co(II)-complexes with trigonal prismatic geometry. 11

Magnetic anisotropy of (NBu₄)[Ni(piv)₃] (2)

Static magnetic data were measured for polycrystalline sample of **2** (Fig. 5), whose powder XRD pattern agrees well with the calculated one (Fig. S2). Its χMT product is 1.30 cm³ K mol⁻¹ at 300 K, which is larger than the theoretical χMT value (1.16 cm³ K mol⁻¹, g = 2.15) for the Ni(II) ion in an octahedral environment with largely quenched orbital moment. The χMT value remains roughly constant in the range of 300-20 K, then decreases abruptly to 0.64 cm³ K mol⁻¹ at 2.0 K. The field-dependent magnetizations of **2** were measured from 1 to 7 T at 2.0, 3.0, and 5.0 K (Fig. 5b). The magnetization continuously increases with the magnetic field and reaches 2.03 $N\beta$ at 7 T at 2.0 K, close to the expected value of 2.0 $N\beta$ (S = 1, g = 2.0).

For six-coordinate Ni(II) complex, the widely used effective spin-Hamiltonian with the axial and rhombic zero-field splitting (ZFS) parameters can be used to present the magnetic anisotropy, 12,16-18 as showed in equation 2:

$$H = D(\hat{S}_z^2 - S(S+1)/3) + E(\hat{S}_x^2 - \hat{S}_y^2) + \mu_B g \hat{S} \cdot \hat{H}$$
 (2)

Here, μ_B denotes the Bohr magneton and D, E, S and B represent the axial and

rhombic ZFS parameters, the spin, and the magnetic field vectors, respectively. The $\chi_M T$ data and magnetization curves were fitted simultaneously using the PHI program.²³ The reasonable fitting results show that the D value is -7.86(4) cm⁻¹ with the corresponding E and g being 0.76(2) cm⁻¹ and 2.440(3), 1.918(4), respectively.

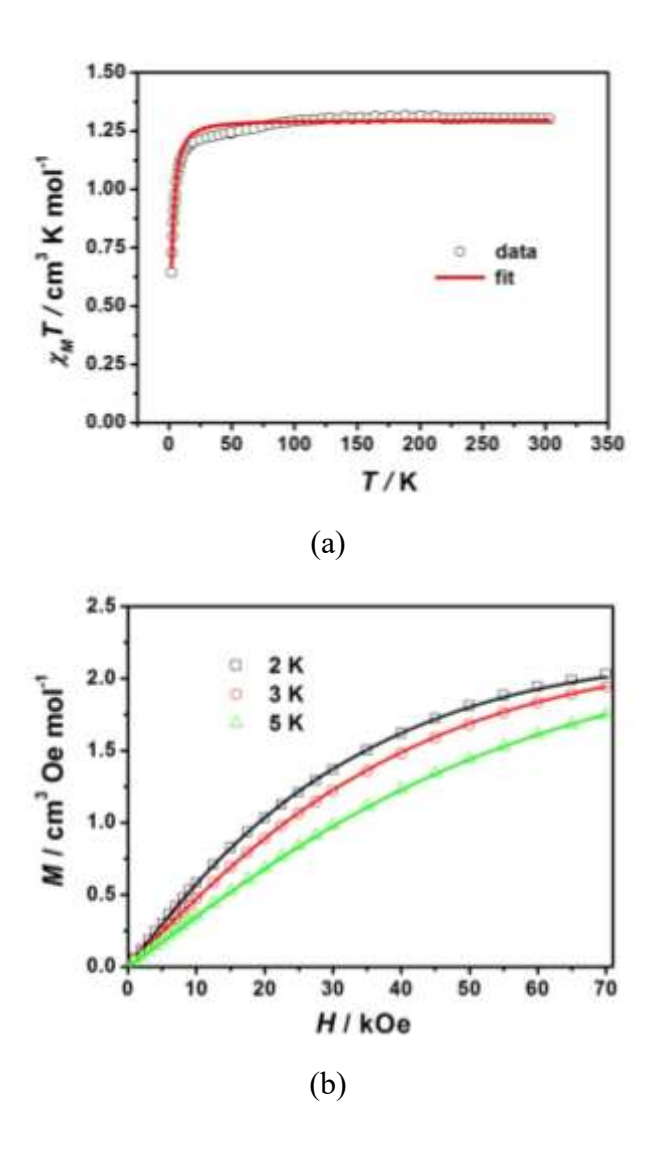


Fig. 5 Variable-temperature dc susceptibility data under an applied dc field of 1000 Oe (a) and field dependent magnetizations (b) for **2**. Solid lines indicate the best fits with *PHI* program.²³

The easy-axial type of magnetic anisotropy of Ni(II) in 2 was further studied by tunable-frequency HFEPR spectra^{17a} with frequency range from 56 to 406 GHz up to 16 T. The spectra are typical of an S = 1 spin state. An EPR spectrum recorded at 302.4 GHz and 4 K is shown in Fig. 6. The main feature of the spectra is a very intense transition at low field, denoted as B_{min} , and the three others being much weaker. The former is due to the off-axis turning point of the forbidden ($\Delta Ms = \pm 2$) transition, which is usually the highest peak in the triplet powder spectrum.²⁶ More information can be derived from the 2D resonating field versus frequency map created from the turning points of the series of EPR spectra (Fig. 7). In the spin-triplet spectrum, three zero-field transitions are possible, which would appear at microwave frequencies of 2|E|, |D|-|E| and |D|+|E|, respectively. In our case, the positions of three zero-field transitions are at nearly 56 GHz (1.87 cm⁻¹), 168 GHz (5.6 cm⁻¹) and 212.8 GHz (7.1 cm⁻¹). Thus the |D| and |E| values can be roughly estimated as 6.4 and 0.94 cm⁻¹, which were used as the initial values to simulate the 2D resonating field versus frequency map (Fig. 7). The best spin Hamiltonian parameters used in the simulations²⁷ are: |D| = 6.61(3) cm⁻¹, E = 0.98(3) cm⁻¹, $g_x = 2.22(2)$, $g_y = 2.22(2)$, and $g_z = 2.25(5)$. In order to reveal the sign of the D value, the EPR spectrum recorded at 302.4 GHz and 4 K was also simulated using the above Hamiltonian parameters. The blue and red traces are the simulated spectra using the positive and negative D values, respectively, which prove a negative D value for 2. These precisely determined D and E values are comparable to those from magnetic data. They are also within the zero-field spitting parameters of the six-coordinate Ni(II) complexes determined by

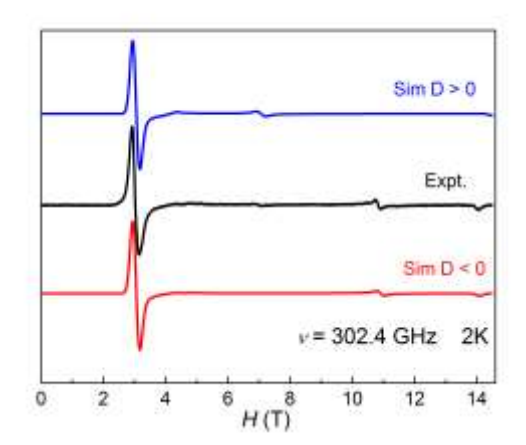


Fig. 6 HF-EPR spectrum of 2 with its simulations at 302.4 GHz and 4 K.

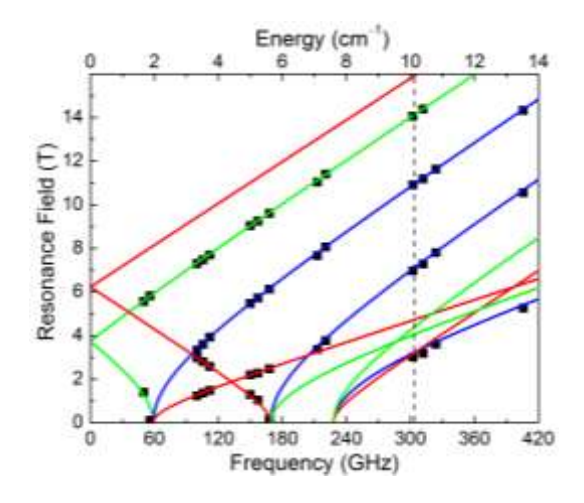


Fig. 7 Resonance field vs microwave frequency (quantum energy) of EPR transitions for **2**. The Hamiltonian parameters used are: S = 1, $g_x = 2.22(2)$, $g_y = 2.22(2)$, $g_z = 2.25(5)$, |D| = 6.61(3) cm⁻¹, E = 0.98(3) cm⁻¹. Green, blue, and red curves are the simulations using the best-fitted spin Hamiltonian parameters with the magnetic field B parallel to the x, y, and z axis of the ZFS tensor, respectively. The vertical dashed line represents the frequency (302.4 GHz) used in Fig. 6 at which the spectra were recorded or simulated.

The zero-field splitting parameters of **2** were also calculated using the MOLCAS 8.2^{25} program package at the XMS-CASPT2 level.²⁴ The calculated D, E (cm⁻¹) and g tensor (x, y, z) of **2** are listed in Table S4, where the calculated D (-7.1 cm⁻¹) and E (1.2 cm⁻¹) values agree well with those determined by HFEPR spectra $(D = -6.61(3), E = 0.98(3) \text{ cm}^{-1})$. The calculated orientations of the g_x , g_y , g_z (hard axis) of the ground doublet on Ni^{II} ion of **2** is shown in Fig. S4. The calculated $\chi_M T$ versus T plot of **2** shown in Fig. S5 agrees well with the experimental curve. These results furthermore support the easy-axis magnetic anisotropy of **2**.

Magnetic relaxation by ac magnetic susceptibility studies

Alternative-current susceptibilities measurements were performed for 1 and 2 in order to study the low temperature dynamic magnetic behavior. No out of phase ac susceptibility (χ_M ") signal was observed for 1 under zero applied dc field at 1.8 K (Fig. S6), which is probably due to the occurrence of quantum tunneling of the magnetization (QTM). The application of an external magnetic field could induce the frequency-dependent ac susceptibilities (Fig. S6), suggesting that the QTM phenomenon could be suppressed. For 1, the maximum of χ_M " appears at 400 Oe, which becomes the strongest with the increasing of the applied magnetic field up to 1000 Oe. Therefore an optimum magnetic field of 1000 Oe was used for temperature-and frequency-dependent ac measurements in the temperature range of 1.8-6.0 K (Figs. 8, S7). A frequency-dependent signal was observed below 6 K as shown in the χ_M " vs T plot (Fig. S7), suggesting slow relaxation of the magnetization, generally

attributed to a SMM behavior.

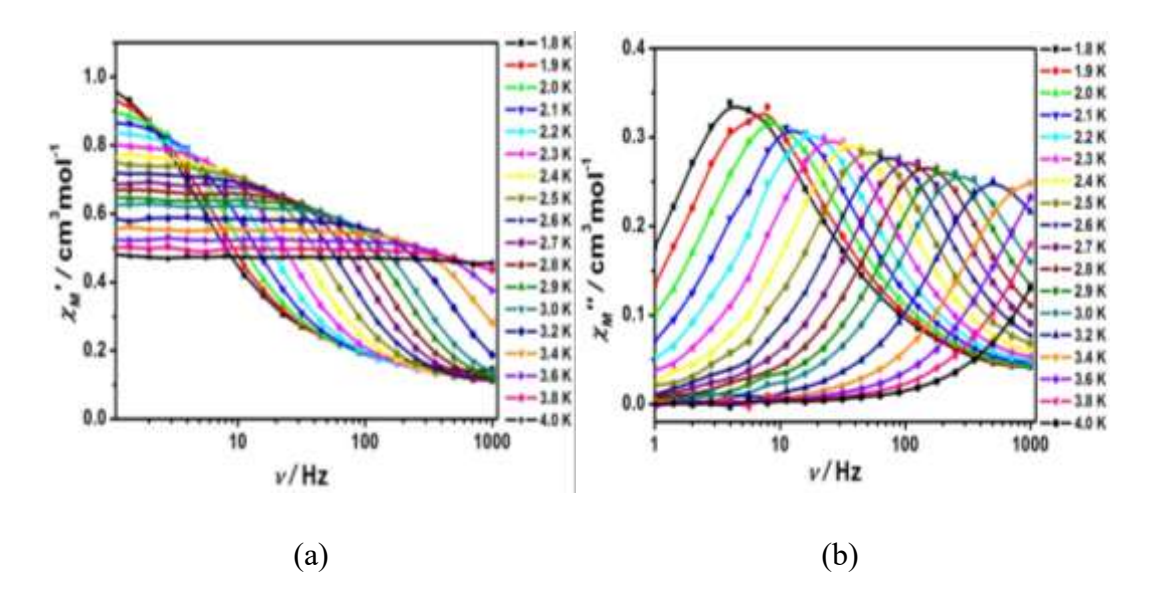


Fig. 8 Frequency dependence of in-phase $(\chi M')$ (a) and out-of-phase $(\chi M'')$ (b) ac magnetic susceptibilities from 1.8 to 4.5 K under 1000 Oe dc field for **1**. The solid lines are for eye guide.

In contrast with 1, no significant χ_M " signals were observed for 2 with the frequency of 1-1000 Hz at 1.8 K using an applied magnetic field in the range of 0-1000 Oe (Fig. S6, right), suggesting that 2 does not exhibit the SIM property at 1.8 K.

The Cole-Cole plots were created from the alternating current data of **1** and fit using the generalized Debye model²⁸ based on equation 3 to extract the values and distribution of the relaxation times:

$$\chi_{ac}(\omega) = \chi_S + \frac{\chi_T - \chi_S}{1 + (i\omega\tau)^{(1-\alpha)}}$$
(3)

where χ_T and χ_S are the isothermal and the adiabatic susceptibility, respectively; ω is angular frequency; τ is the relaxation time; α indicates deviation from a pure Debye model.²⁸ As shown in Fig. 9, the Cole-Cole plots of χ_M " $vs \chi_M$ between 1.8 and 4.0 K have semicircular profiles, indicative of a single relaxation process. The fitting parameters are summarized in Table S5. The parameter α is in the range of 0.00-0.25 and is found to increase with the decrease of temperature, suggesting a small distribution of relaxation times.

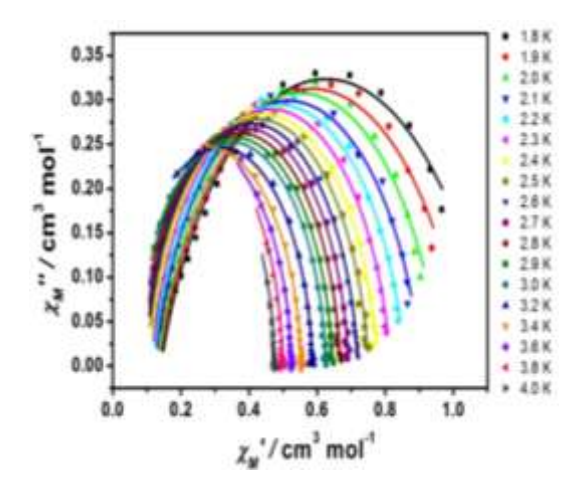


Fig. 9 Cole-Cole plot obtained from the ac susceptibility data under 1000 Oe dc field between 1.8 and 4.0 K for 1. Solid lines represent the best fits to a generalized Debye model.

The obtained values of relaxation time in the range 1.8 to 4.0 K were fit by the Arrhenius law $\tau = \tau_0 \exp(U_{\rm eff}/kT)$ to give $U_{\rm eff} = 20.8 \ {\rm cm}^{-1}$ ($\tau_0 = 2.53 \times 10^{-8} \ {\rm s}$) for 1 (Fig. S8). This derivation of the effective energy barrier was based on the assumption that the dominant relaxation mechanism is the thermally activated Orbach process in the studied temperature range. In fact, the Orbach mechanism is not the necessarily

dominant process, at least in the investigated temperature range. In the Arrhenius plot of 1, the obvious curvature implies that non-negligible Raman process contributes the relaxation rate. On this ground, a model including Orbach and Raman mechanisms was used to analysize the contribution to the relaxation rate in 1 by given equation 4:²⁹

$$\tau^{-1} = CT^n + \tau_0^{-1} \exp(-U_{eff}/kT)$$
 (4)

Here, the two terms represent the contributions of the Raman and Orbach processes, respectively. The best fitting results of the relaxation time vs temperature curves give the following parameters: n = 5.6, $C = 1.19 \text{ s}^{-1} \text{ K}^{-5.6}$, $\tau_0 = 1.4 \times 10^{-8} \text{ s}$, and $U_{eff} = 22.7 \text{ cm}^{-1}$. The fit reproduces the experimental data very well (Fig. S9). The using of Orbach model implies that an excited state exists at an energy separation of 22.7 cm⁻¹ above the ground state to provide the intermediate state in the relaxation process. But the first excited state is theoretically predicted to be 167.7 cm⁻¹ higher than the ground state for 1. Therefore the Orbach process is unlikely to be involved in the magnetic relaxation in 1. When the Orbach mechanism is neglected, the relaxation time data could be fit by a power law $\tau^{-1} = CT^n$ to give the resulting values n = 8.5 and $C = 0.16 \text{ s}^{-1} \text{ K}^{-8.5}$ (Fig. 10). The obtained n value is very close to the expected n = 9 for Raman mechanism in Kramers ions, suggesting the dominant contribution of a Raman process for the spin relaxation in 1.29

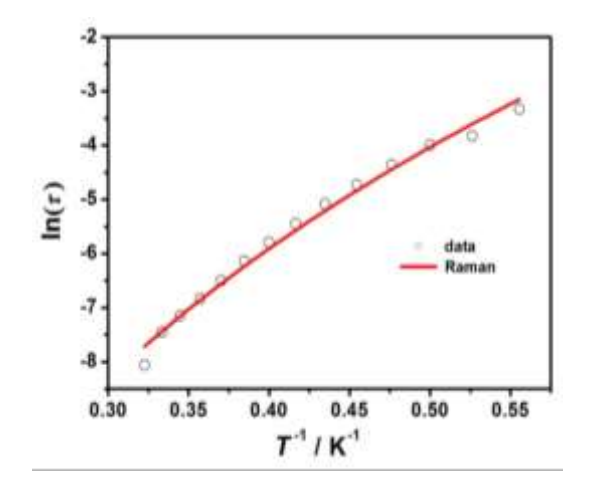


Fig. 10 $ln(\tau)$ *vs* ln(T) plot of complex 1.

Conclusions

The static and dynamic magnetic studies have been performed on mononuclear, six-coordinated Co(II) and Ni(II) complexes (NBu₄)[M(piv)₃] (piv = pivalate, M = Co, 1; M = Ni, 2) with a configuration at the midway between the octahedron and trigonal prismatic geometry. The joint studies employing the magnetic measurement, HFEPR spectroscopy and theoretical calculations confirm the negative sign of magnetic anisotropy in 1 and 2. The ac magnetic susceptibility data show that 1 is a field-induced SIM, but 2 does not slow magnetic relaxation at 1.8 K. While the six-coordinate Co(II) complexes with positive magnetic anisotropy are well studied, the examples of the complexes exhibiting field-induced SIM properties due to the negative magnetic anisotropy are relatively scarce. This work adds a new number of six-coordinate Co(II)-based field-induced SIM with negative magnetic anisotropy.

Conflicts of interest

There are no conflicts to declare.

Acknowledgements

We are grateful for the financial support from the Natural Science Grant of China (No. 21471078 to XTC, and 11774178 to YQZ), and the US National Science Foundation (CHE-1633870 to ZLX).

Notes and references

- (a) D. Gatteschi and R. Sessoli, Angew. Chem., Int. Ed., 2003, 42, 268; (b) W.
 Wernsdorfer and R. Sessoli, Science, 1999, 284, 133; (c) M. N. Leuenberger and D. Loss, Nature, 2001, 410, 789; (d) R. E. P. Winpenny, Angew. Chem., Int. Ed., 2008, 47, 7992; (e) D. Gatteschi, R. Sessoli and J. Villain, Molecular Nanomagnets, Oxford University Press, Oxford, UK, 2006.
- (a) R. Sessoli, H. L. Tsai, A. R. Schake, S. Wang, J. B. Vincent, K. Folting, D. Gatteschi, G. Christou and D. N. Hendrickson, J. Am. Chem. Soc., 1993, 115, 1804; (b) R. Sessoli, D. Gatteschi, A. Caneschi and M. A. Novak, Nature, 1993, 365, 141; (c) R. Bagai, G.Christou, Chem. Soc. Rev., 2009, 38, 1011; (d) D. Gatteschi, R. Sessoli, A. Cornia, Chem. Commun., 2000, 725; (e) K. S. Pedersen, J. Bendix, R. Clérac, Chem. Commun., 2014, 50, 4396; (f) M. Murrie, Chem. Soc. Rev., 2010, 39, 1986.
- 3 (a) D. N. Woodruff, R. E. P. Winpenny, R. A. Layfield, *Chem. Rev.*, 2013, 113,
 5110; (b) H. L. C. Feltham, S. Brooker, *Coord. Chem. Rev.*, 2014, 276, 1.
- 4 N. Magnani and R. Caciuffo, *Inorganics*, 2018, **6**, 26.
- 5 (a) G. A. Craig and M. Murrie, Chem. Soc. Rev. 2015, 44, 2135; (b) A. K. Bar, C.

- Pichon and J.-P. Sutter, *Coord. Chem. Rev.*, 2016, **308**, 346; (*c*) J. M. Frost, K. L. M. Harriman and M. Murugesu, *Chem. Sci.*, 2016, **7**, 2470; (*d*) M. Atanasov, D.Aravena, E. Suturina, E. Bill, D. Maganas and F. Neese, *Coord. Chem. Rev.*, 2015, **289–290**, 177; (*e*) S. Gómez-Coca, D. Aravena, R. Morales and E. Ruiz, *Coord. Chem. Rev.*, 2015, **289–290**, 379.
- 6 D. E. Freedman, W. H. Harman, T. D. Harris, G. J. Long, C. J. Chang and J. R. Long, J. Am. Chem. Soc., 2010, 132, 1224.
- 7 (a) J. Vallejo, A. Pascual-Álvarez, J. Cano, I. Castro, M. Julve, F. Lloret, J. Krzystek, G. D. Munno, D. Armentano, W. Wernsdorfer, R. Ruiz-García and E. Pardo, *Angew. Chem. Int. Ed.*, 2013, **52**, 14075; (b) M. Ding, G. E. Cutsail III, D. Aravena, M. Amoza, M. Rouzières, P. Dechambenoit, Y. Losovyj, M. Pink, E. Ruiz, R. Clérac and J. M. Smith, *Chem. Sci.*, 2016, **7**, 6132.
- 8 (a) J. M. Zadrozny, D. J. Xiao, M. Atanasov, G. J. Long, F. Grandjean, F. Neese and J. R. Long, Nat. Chem., 2013, 5, 577; (b) M. Atanasov, J. M. Zadrozny, J. R. Long and F. Neese, Chem. Sci., 2013, 4, 139; (c) A. K. Bar, C. Pichon, N. Gogoi, C. Duhayon, S. Ramasesha and J.-P. Sutter, Chem. Commun., 2015, 51, 3616; (d) S. Mossin, B. L. Tran, D. Adhikari, M. Pink, F. W. Heinemann, J. Sutter, R. K. Szilagyi, K. Meyer and D. J. Mindiola, J. Am. Chem. Soc., 2012, 134, 13651.
- (a) Y.-S. Meng, Z. Mo, B.-W. Wang, Y.-Q. Zhang, L. Deng and S. Gao, *Chem. Sci.*, 2015, 6, 7156; (b) X.-N. Yao, J.-Z. Du, Y.-Q. Zhang, X.-B. Leng, M.-W. Yang, S.-D. Jiang, Z.-X. Wang, Z.-W. Ouyang, L. Deng, B.-W. Wang and S. Gao, *J. Am. Chem. Soc.*, 2017, 139, 373; (c) A. Eichhöfer, Y. Lan, V. Mereacre, T. Bodenstein

and F. Weigend, *Inorg. Chem.*, 2014, **53**, 1962; (*d*) S. Gomez-Coca, E. Cremades, N. Aliaga-Alcalde and E. Ruiz, *J. Am. Chem. Soc.*, 2013, **135**, 7010; (*e*) F. Habib, O. R. Luca, V. Vieru, M. Shiddiq, I. Korobkov, S. I. Gorelsky, M. K. Takase, L. F. Chibotaru, S. Hill, R. H. Crabtree and M. Murugesu, *Angew. Chem.*, *Int. Ed.*, 2013, **52**, 11290; (*f*) D. Schweinfurth, M. G. Sommer, M. Atanasov, S. Demeshko, S. Hohloch, F. Meyer, F. Neese and B. Sarkar, *J. Am. Chem. Soc.*, 2015, **137**, 1993; (*g*) P. Antal, B. Drahoš, R. Herchel and Z. Trávníček, *Inorg. Chem.* 2016, **55**, 5957; (*h*) L. Chen, H.-H. Cui, S. E. Stavretis, S. C. Hunter, Y.-Q. Zhang, X.-T. Chen, Y.-C. Sun, Z. Wang, Y. Song, A. A. Podlesnyak, Z.-W. Ouyang and Z.-L. Xue, *Inorg. Chem.*, 2016, **55**, 12603; (*i*) L. Chen, J. Wang, J.-M. Wei, W. Wernsdorfer, X.-T. Chen, Y.-Q. Zhang, Y. Song and Z.-L. Xue, *J. Am. Chem. Soc.*, 2014, **136**, 12213.

(a) J. Vallejo, I. Castro, R. Ruiz-García, J. Cano, M. Julve, F. Lloret, G. De Munno, W. Wernsdorfer and E. Pardo, J. Am. Chem. Soc., 2012, 134, 15704; (b)
E. Colacio, J. Ruiz, E. Ruiz, E. Cremades, J. Krzystek, S. Carretta, J. Cano, T. Guidi, W. Wernsdorfer and E. K. Brechin, Angew. Chem., Int. Ed. 2013, 52, 9130; (c) V. Chandrasekhar, A. Dey, A. J. Mota and E. Colacio, Inorg. Chem., 2013, 52, 4554; (d) D. Y. Wu, X. X. Zhang, P. Huang, W. Huang, M. Y. Ruan and Z. W. Ouyang, Inorg. Chem., 2013, 52, 10976; (e) S. Gómez-Coca, A. Urtizberea, E. Cremades, P. J. Alonso, A. Camón, E. Ruiz and F. Luis, Nat. Commun., 2014, 5, 4300; (f) R. Herchel, L. Váhovská, I. Potočňák and Z. Trávníček, Inorg. Chem., 2014, 53, 5896; (g) J. Li, Y. Han, F. Cao, R.-M. Wei, Y.-Q. Zhang and Y. Song,

Dalton Trans., 2016, 45, 9279; (h) Y.-Z. Zhang, S. Gómez-Coca, A. J. Brown, M. R. Saber, X. Zhang and K. R. Dunbar, Chem. Sci., 2016, 7, 6519; (i) R. Díaz-Torres, M. Menelaou, O. Roubeau, A. Sorrenti, G. Brandariz-de-Pedro, E. C. Saňudo, S. J. Teat, J. Fraxedas, E. Ruiz and N. Aliaga-Alcalde, Chem. Sci., 2016, 7, 2793; (j) A. Świtlicka-Olszewska, J. Palion-Gazda, T. Klemens, B. Machura, J. Vallejo, J. Cano, F. Lloret and M. Julve, *Dalton Trans.*, 2016, **45**, 10181; (k) D. V. Korchagin, A. V. Palii, E. A. Yureva, A. V. Akimov, E. Y. Misochko, G. V. Shilov, A. D. Talantsev, R. B. Morgunov, A. A. Shakin, S. M. Aldoshin and B. S. Tsukerblat, *Dalton Trans.*, 2017, **46**, 7540; (*l*) A. V. Palii, D. V. Korchagin, E. A. Yureva, A. V. Akimov, E. Y. Misochko, G. V. Shilov, A. D. Talantsev, R. B. Morgunov, S. M. Aldoshin and B. S. Tsukerblat, *Inorg. Chem.*, 2016, 55, 9696; (m) J. P. S. Walsh, G. Bowling, A.-M. Ariciu, N. F. M. Jailani, N. F. Chilton, P. G. Waddell, D. Collison, F. Tuna and L. J. Higham, Magnetochem., 2016, 2, 23; (n) L. Chen, J. Zhou, H.-H. Cui, A.-H. Yuan, Z. Wang, Y.-Q. Zhang, Z.-W. Ouyang and Y. Song, Dalton Trans., 2018, 47, 2506.

(a) Y.-Y. Zhu, C. Cui, Y.-Q. Zhang, J.-H. Jia, X. Guo, C. Gao, K. Qian, S.-D. Jiang, B.-W. Wang, Z.-M. Wang and S. Gao, *Chem. Sci.*, 2013, 4, 1802; (b) Y.-Y. Zhu, Y.-Q. Zhang, T.-T. Yin, C. Gao, B.-W. Wang and S. Gao, *Inorg. Chem.*, 2015, 54, 5475; (c) V. V. Novikov, A. A. Pavlov, Y. V. Nelyubina, M.-E. Boulon, O. A. Varzatskii, Y. Z. Voloshin and R. E. P. Winpenny, *J. Am. Chem. Soc.*, 2015, 137, 9792; (d) A. A. Pavlov, Y. V. Nelyubina, S. V. Kats, L. V. Penkova, N. N. Efimov, A. O. Dmitrienko, A. V. Vologzhanina, A. S. Belov, Y. Z. Voloshin and V.

- V. Novikov, *J. Phys. Chem. Lett.*, 2016, **7**, 4111; (*e*) Y. Peng, T. Bodenstein, K. Fink, V. Mereacre, C. E. Ansona and A. K. Powell, *Phys. Chem. Chem. Phys.*, 2016, **18**, 30135; (*f*) T. J. Ozumerzifon, I. Bhowmick, W. C. Spaller, A. K. Rappe and M. P. Shores, *Chem. Commun.*, 2017, **53**, 4211; (*g*) S. Gomez-Coca, E. Cremades, N. Aliaga-Alcalde and E. Ruiz, *J. Am. Chem. Soc.*, 2013, **135**, 7010.
- 12 (a) W. Lin, T. Bodenstein, V. Mereacre, K. Fink and A. Eichhöfer, *Inorg. Chem.*, 2016, 55, 2091; (b) K. E. R. Marriott, L. Bhaskaran, C. Wilson, M. Medarde, S. T. Ochsenbein, S. Hill and M. Murrie, *Chem. Sci.*, 2015, 6, 6823; (c) J. Miklovič, D. Valigura, R. Boča and J.Titiš, *Dalton Trans.*, 2015, 44, 12484; (d) D. Lomjanský, J. Moncol', C. Rajnák, J. Titiš and R. Boča, *Chem. Commun.*, 2017, 53, 6930.
- 13 R. Boča, C. Rajnák, J. Titiš and D. Valigura, *Inorg. Chem.*, 2017, **56**, 1478.
- 14 (a) Y.-F. Deng, T. Han, Z. Wang, Z. Ouyang, B. Yin, Z. Zheng, J. Krzystek and Y.-Z. Zheng, Chem. Commun., 2015, 51, 17688; (b) A. Cornia, L. Rigamonti, S. Boccedi, R. Clérac, M. Rouzières and L. Sorace, Chem. Commun., 2014, 50, 15191.
- 15 (a) J. Martínez-Lillo, T. F. Mastropietro, E. Lhotel, C. Paulsen, J. Cano, G. D. Munno, J. Faus, F. Lloret, M. Julve, S. Nellutla and J. Krzystek, *J. Am. Chem. Soc.*, 2013, 135, 13737; (b) K. S. Pedersen, M. Sigrist, M. A. Sørensen, A.-L. Barra, T. Weyhermiiller, S. Piligkos, C. A. Thuesen, M. G. Vinum, H. Mutka, H. Weihe, R. Clérac and J. Bendix, *Angew. Chem. Int. Ed.*, 2014, 53, 1351.
- 16 (a) S.-D. Jiang, D. Maganas, N. Levesanos, E. Ferentinos, S. Haas, K. Thirunavukkuarasu, J. Krzystek, M. Dressel, L. Bogani, F. Neese and P. Kyritsis,

- J. Am. Chem. Soc., 2015, 137, 12923; (b) S. Gómez-Coca, E. Cremades, N.
 Aliaga-Alcalde and E. Ruiz, Inorg. Chem., 2014, 53, 676; (c) R. Ruamps, R.
 Maurice, L. Batchelor, M. Boggio-Pasqua, R. Guillot, A. L. Barra, J. Liu, E.-E.
 Bendeif, S. Pillet, S. Hill, T. Mallah and N. Guihéry, J. Am. Chem. Soc., 2013,
 135, 3017; (d) R. Ruamps, L. J. Batchelor, R. Maurice, N. Gogoi, P.
 Jiménez-Lozano, N. Guihéry, C. de Graaf, A.-L. Barra, J.-P. Sutter and T. Mallah,
 Chem. -Eur. J., 2013, 19, 950; (e) I. Nemec, R. Herchel, I. Svoboda, R. Boča and
 Z. Trávníček, Dalton Trans., 2015, 44, 9551.
- 17 (a) J. Krzystek, S. A. Zvyagin, A. Ozarowski, S. Trofimenko and J. Telser, J. Magn. Reson., 2006, 178, 174; (b) J. Krzystek, J.-H. Park, M. W. Meisel, M. A. Hitchman, H. Stratemeier, L.-C. Brunel and J. Telser, Inorg. Chem., 2002, 41, 4478; (c) P. J. Desrochers, J. Telser, S. A. Zvyagin, A. Ozarowski, J. Krzystek and D. A. Vicic, Inorg. Chem., 2006, 45, 8930; (d) I. Nieto, R. P. Bontchev, A. Ozarowski, D. Smirnov, J. Krzystek, J. Telser, J. M. Smith, Inorg. Chim. Acta, 2009, 362, 4449; (e) J.-N. Rebilly, G. Charron, E. Rivière, R. Guillot, A.-L. Barra, M. D. Serrano, J. van Slageren and T. Mallah, Chem. Eur. J., 2008, 14, 1169; (f) B. Cahier, M. Perfetti, G. Zakhia, D. Naoufal, F. El-Khatib, R. Guillot, E. Rivière, R. Sessoli, A.-L. Barra, N. Guihéry and T. Mallah, Chem. Eur. J., 2017, 23, 3648.
- 18 (a) J. Krzystek, A. Ozarowski and J. Telser, Coord. Chem. Rev., 2006, 250, 2308;(b) G. Rogez, J.-N. Rebilly, A.-L. Barra, L. Sorace, G. Blondin, N. Kirchner, M. Duran, J. van Slageren, S. Parsons, L. Ricard, A. Marvilliers and T. Mallah,

Angew. Chem. Int. Ed., 2005, 44, 1876; (c) D. Dobrzyńska, L. B. Jerzykiewicz,
M. Duczmal, A. Wojciechowska, K. Jabłońska, J. Palus and A. Ozarowski, Inorg. Chem., 2006, 45, 10479; (d) G. Charron, F. Bellot, F. Cisnetti, G. Pelosi, J.-N.
Rebilly, E. Rivère, A.-L. Barra, T. Mallah and C. Policar, Chem. Eur. J., 2007,
13, 2774; (e) A. Wojciechowska, M. Daszkiewicz, Z. Staszak, A. Trusz-Zdybek,
A. Bieńko and A. Ozarowskiz, Inorg. Chem., 2011, 50, 11532; (f) D. Maganas, J.
Krzystek, E. Ferentinos, A. M. Whyte, N. Robertson, V. Psycharis, A. Terzis, F.
Neese and P. Kyritsis, Inorg. Chem., 2012, 51, 7218; (g) D. Schweinfurth, J.
Krzystek, I. Schapiro, S. Demeshko, J. Klein, J. Telser, A. Ozarowski, C.-Y. Su,
F. Meyer, M. Atanasov, F. Neese and B. Sarkar, Inorg. Chem., 2013, 52, 6880;
(h) A. Wojciechowska, J. Janczak, Z. Staszak, M. Duczmal, W. Zierkiewicz, J.
Tokar and A. Ozarowski, New J. Chem., 2015, 39, 6813; (i) G. Charron, E.
Malkin, G. Rogez, L. J. Batchelor, S. Mazerat, R. Guillot, N. Guihéry, A.-L.
Barra, T. Mallah and H. Bolvin, Chem. Eur. J., 2016, 22, 16850.

- 19 (a) E. Fursova, G. Romanenko, R. Sagdeev and V. Ovcharenko, *Polyhedron*, 2014, **81**, 27; (b) E. Fursova, G. Romanenko and V. Ovcharenko, *Polyhedron*, 2013, **62**, 274.
- (a) M. Llunell, D. Casanova, J. Cirera, P. Alemany and S. Alvarez, *Shape Program*, Version 2.1, 2013; (b) S. Alvarez, P. Alemany, D. Casanova, J. Cirera, M. Llunell and D. Avnir, *Coord. Chem. Rev.*, 2005, 249, 1693.
- 21 F. E. Mabbs and D. J. Machin, *Magnetism and Transition Matal Complexes*,
 Dover Publications: Mineola, NY, 2008.

- 22 (*a*) F. Lloret, M. Julve, J. Cano, R. Ruiz-García and E. Pardo, *Inorg. Chim. Acta*, 2008, 361, 3432; (b) J. Titiš and R. Boča, *Inorg. Chem.*, 2011, **50**, 11838.
- 23 N. F. Chilton, R. P. Anderson, L. D. Turner, A. Soncini and K. S. Murray, *J. Comput. Chem.*, 2013, **34**, 1164.
- G. Karlström, R. Lindh, P. -Å. Malmqvist, B. O. Roos, U. Ryde, V. Veryazov, P.
 -O. Widmark, M. Cossi, B. Schimmelpfennig, P. Neogrady and L. Seijo, *Comput. Mater. Sci.*, 2003, 28, 222.
- 25 L. Ungur and L. F. Chibotaru. Chem. Eur. J., 2017, 23, 3708.
- 26 F. E. Mabbs and D. Collison, Electron Paramagnetic Resonance of Transition Metal Compounds, Elsevier, Amsterdam, 1992.
- 27 Simulations were performed using SPIN developed by Andrew Ozarowski in National High Magnetic Field Laboratory, US.
- 28 (a) Y.-N. Guo, G.-F. Xu, Y. Guo and J. Tang, *Dalton Trans.*, 2011, 40, 9953; (b)K. S. Cole and R. H. Cole, *J. Chem. Phys.*, 1941, 9, 341.
- 29 (a) R. L. Carlin and A. J. van Duyneveldt, Magnetic Properties of Transition Metal compounds, Springer-Verlag, New York, 1976; (b) K.N. Shrivastava, Phys. Status Solidi B, 1983, 117, 437.